
THE NON-IID DATA QUAGMIRE OF DECENTRALIZED MACHINE LEARNING

Kevin Hsieh¹ Amar Phanishayee² Onur Mutlu^{3,1} Phillip B. Gibbons¹

¹ Carnegie Mellon University ² Microsoft Research ³ ETH Zürich

ABSTRACT

Many large-scale machine learning (ML) applications need to train ML models over *decentralized* datasets that are generated at different devices and locations. These decentralized datasets pose a fundamental challenge to ML because they are typically generated in very different contexts, which leads to significant differences in data distribution across devices/locations (i.e., they are *not* independent and identically distributed (IID)). In this work, we take a step toward better understanding this challenge, by presenting the first detailed experimental study of the impact of such *non-IID data* on the decentralized training of deep neural networks (DNNs). Our study shows that: (i) the problem of non-IID data partitions is fundamental and pervasive, as it exists in all ML applications, DNN models, training datasets, and decentralized learning algorithms in our study; (ii) this problem is particularly difficult for DNN models with batch normalization layers; and (iii) the degree of deviation from IID (the skewness) is a key determinant of the difficulty level of the problem. With these findings in mind, we present SkewScout, a system-level approach that adapts the communication frequency of decentralized learning algorithms to the (skew-induced) accuracy loss between data partitions. We also show that group normalization can recover much of the skew-induced accuracy loss of batch normalization.

1 INTRODUCTION

The advancement of machine learning (ML) is heavily dependent on the processing of massive amounts of data. The most timely and relevant data are often generated at different devices all over the world, e.g., data collected by mobile phones and video cameras. Because of communication and privacy constraints, gathering all these data for centralized processing is impractical/infeasible, motivating the need for ML training over widely distributed data (*decentralized learning*). For example, *geo-distributed learning* (Hsieh et al., 2017) trains a global ML model over data spread across geo-distributed data centers. Similarly, *federated learning* (McMahan et al., 2017) trains a centralized model over data from a large number of devices (mobile phones).

Key Challenges in Decentralized Learning. There are two key challenges in decentralized learning. First, training a model over decentralized data using traditional training approaches (i.e., those designed for centralized data) requires massive communication, which drastically slows down the training process because the communication is bottlenecked by the limited wide-area or mobile network bandwidth (Hsieh et al., 2017; McMahan et al., 2017). Second, decentralized data are typically generated at different contexts, which can lead to significant differences in the *distribution* of the data across data partitions. For example, facial images collected by cameras will reflect the demographics of each camera’s location, and images of kangaroos

will be collected only from cameras in Australia or zoos. Unfortunately, existing decentralized learning algorithms (e.g., (Hsieh et al., 2017; McMahan et al., 2017; Smith et al., 2017; Lin et al., 2018; Tang et al., 2018)) mostly focus on reducing communication, as they either (i) assume that data are independent and identically distributed (IID) across different partitions or (ii) conduct only a very limited study on non-IID data partitions. This leaves a key question mostly unanswered: *What happens to different ML applications and decentralized learning algorithms when their training data partitions are not IID?*

Our Goal and Key Findings. In this work, we aim to answer the above key question by conducting the first detailed empirical study of the impact of non-IID data partitions on decentralized learning. Our study covers various ML applications, ML models, training datasets, decentralized learning algorithms, and degrees of deviation from IID. We focus on deep neural networks (DNNs) as they are the most relevant solutions for our applications. Our study reveals three key findings:

- Training over non-IID data partitions is a fundamental and pervasive problem for decentralized learning. All three decentralized learning algorithms in our study suffer from major model quality loss (or even divergence) when run on non-IID data partitions, across *all* applications, models, and training datasets in our study.
- DNNs with *batch normalization* (Ioffe & Szegedy, 2015)

are particularly vulnerable to non-IID data partitions, suffering significant model quality loss even under BSP, the most communication-heavy approach to decentralized learning.

- The degree of deviation from IID (the *skewness*) is a key determinant of the difficulty level of the problem.

These findings reveal that non-IID data is an important yet heavily understudied challenge in decentralized learning, worthy of extensive study.

Solutions. As two initial steps towards addressing this vast challenge, we first show that among the many proposed alternatives to batch normalization, *group normalization* (Wu & He, 2018) avoids the skew-induced accuracy loss of batch normalization under BSP. With this fix, all models in our study perform well under BSP for non-IID data, and the problem can be viewed as a trade-off between accuracy and communication frequency. Intuitively, there is a tug-of-war among the different data partitions, with each partition pulling the model to reflect its data, and only frequent communication, tuned to the skew-induced accuracy loss, can save the overall model accuracy of the algorithms in our study. Accordingly, we present SkewScout, a system-level approach that adapts the communication frequency of decentralized learning algorithms to accuracy loss, by cross-validating model accuracy across data partitions (*model traveling*). Our experimental results show that SkewScout’s adaptive approach automatically reduces communication by $9.6\times$ (under high skew) to $34.1\times$ (under mild skew) while retaining the accuracy of BSP.

Contributions. We make the following contributions. First, we conduct a detailed empirical study on the problem of non-IID data partitions. To our knowledge, this is the first study to show that the problem of non-IID data partitions is a fundamental and pervasive challenge for decentralized learning. Second, we make a new observation showing that the challenge of non-IID data partitions is particularly problematic for DNNs with batch normalization, even under BSP. We discuss the root cause of this problem and we find that it can be addressed by using an alternative normalization technique. Third, we show that the difficulty level of this problem varies with the data skew. Finally, we design and evaluate SkewScout, a system-level approach that adapts the communication frequency to reflect the skewness in the data, seeking to maximize communication savings while preserving model accuracy.

Our study focuses on *label-based* partitioning of data, in which the distribution of labels varies across partitions. The paper concludes with a broader taxonomy of regimes of non-IID data (§9), the study of which is left to future work.

2 BACKGROUND AND SETUP

We provide background on decentralized learning and popular algorithms for this learning setting (§2.1) and then

describe our study’s experimental setup (§2.2).

2.1 Decentralized Learning

In a decentralized learning setting, we aim to train a ML model w based on all the training data samples (x_i, y_i) that are generated and stored in one of the K partitions (denoted as P_k). The goal of the training is to fit w to all data samples. Typically, most decentralized learning algorithms assume the data samples are independent and identically distributed (IID) among different P_k , and we refer to such a setting as the *IID setting*. Conversely, we call it the *Non-IID setting* if such an assumption does not hold.

We evaluate three popular decentralized learning algorithms to see how they perform on different applications over the IID and Non-IID settings. These algorithms can be used with a variety of stochastic gradient descent (SGD) approaches, and aim to reduce communication, either among data partitions (P_k) or between the data partitions and a centralized server.

- Gaia (Hsieh et al., 2017), a geo-distributed learning algorithm that dynamically eliminates insignificant communication among data partitions. Each partition P_k accumulates updates Δw_j to each model weight w_j locally, and communicates Δw_j to all other data partitions only when its relative magnitude exceeds a predefined threshold (Algorithm 1 in Appendix A)
- FederatedAveraging (McMahan et al., 2017), a popular algorithm for federated learning that combines local SGD on each client with model averaging. Specifically, FederatedAveraging selects a subset of the partitions P_k in each epoch, runs a prespecified number of local SGD steps on each selected P_k , and communicates the resulting models back to a centralized server. The server averages all these models and uses the averaged w as the starting point for the next epoch (Algorithm 2 in Appendix A).
- DeepGradientCompression (Lin et al., 2018), a popular algorithm that communicates only a pre-specified amount of gradients each epoch, with various techniques to retain model quality such as momentum correction, gradient clipping (Pascanu et al., 2013), momentum factor masking, and warm-up training (Goyal et al., 2017) (Algorithm 3 in Appendix A).

In addition to these decentralized learning algorithms, we also show the results of using BSP (bulk synchronous parallel) (Valiant, 1990) over the IID and Non-IID settings. BSP is significantly slower than the above algorithms because it does not seek to reduce communication: All updates from each P_k are accumulated and shared among all data partitions after each training iteration (epoch). As noted earlier, for decentralized learning, there is a natural tension between the frequency of communication and the quality of the resulting model: differing distributions among the

P_k pull the model in different directions—more frequent communication helps mitigate this “tug-of-war” in order that the model well-represents all the data. Thus, BSP, with its full communication every iteration, is used as the target baseline for model quality for each application.

2.2 Experimental Setup

Our study consists of three dimensions: (i) ML applications/models, (ii) decentralized learning algorithms, and (iii) degree of deviation from IID. We explore all three dimensions with rigorous experimental methodologies. In particular, we make sure the accuracy of our trained ML models on IID data matches the reported accuracy in corresponding papers. To our knowledge, this is the first detailed empirical study on ML over non-IID data partitions.

Applications. We evaluate different deep learning applications, DNN model structures, and training datasets:

- **IMAGE CLASSIFICATION** with four DNN models (AlexNet (Krizhevsky et al., 2012), GoogLeNet (Szegedy et al., 2015), LeNet (Lecun et al., 1998), and ResNet (He et al., 2016)) over two datasets (CIFAR-10 (Krizhevsky, 2009) and ImageNet (Russakovsky et al., 2015)). We use the validation data accuracy as the model quality metric.
- **FACE RECOGNITION** with the center-loss face model (Wen et al., 2016) over the CASIA-WebFace (Yi et al., 2014) dataset. We use verification accuracy on the LFW dataset (Huang et al., 2007) as the model quality metric.

For all applications, we tune the training parameters (e.g., learning rate, minibatch size, number of epochs, etc.) such that the baseline model (BSP in the IID setting) achieves the model quality of the original paper. We then use these training parameters in all other settings. We further ensure that training/validation accuracy has stopped improving by the end of all our experiments. Appendix B lists all major training parameters in our study.

Non-IID Data Partitions. We create non-IID data partitions by partitioning datasets using the *labels* on the data, i.e., using image class for image classification and person identities for face recognition. This partitioning emulates real-world non-IID settings, which often involve highly unbalanced label distributions across different locations (e.g., kangaroos only in Australia or zoos, a person’s face in only a few locations worldwide). We control the degree of deviation from IID by controlling the fraction of data that are non-IID. For example, 20% non-IID indicates 20% of the dataset are partitioned by labels, while the remaining 80% are partitioned randomly.

Hyper-Parameters Selection. The algorithms we study provide the following hyper-parameters (see Appendix A for the detail of these algorithms) to control the amount of communication (and hence the training time):

- Gaia uses T_0 , the initial threshold to determine if a

Δw_j is significant. Starting with this initial T_0 , the significance threshold decreases whenever the learning rate decreases.

- FederatedAveraging uses $Iter_{Local}$ to control the number of local SGD steps on each selected P_k .
- DeepGradientCompression uses s to control the sparsity of updates (update magnitudes in top s percentile are exchanged). Following the original paper (Lin et al., 2018), s follows a warm-up scheduling: 75%, 93.75%, 98.4375%, 99.6%, 99.9%. We use a hyper-parameter E_{warm} , the number of epochs for each warm-up sparsity, to control the duration of the warm-up. For example, if $E_{warm} = 4$, s is 75% in epochs 1–4, 93.75% in epochs 5–8, 98.4375% in epochs 9–12, 99.6% in epochs 13–16, and 99.9% in epochs 17+.

We select a hyper-parameter θ of each decentralized learning algorithms (T_0 , $Iter_{Local}$, E_{warm}) so that (i) θ achieves the same model quality as BSP in the IID setting and (ii) θ achieves similar communication savings across the three decentralized learning algorithms. We study the sensitivity of our findings to the choice of θ in §4.2.

3 NON-IID STUDY: RESULTS OVERVIEW

This paper seeks to answer the question as to what happens to ML applications, ML models, and decentralized learning algorithms when their training data partitions are not IID. In this section, we provide an overview of our findings, showing that non-IID data partitions cause *major model quality loss*, across all applications, models, and algorithms in our study. We discuss the results for IMAGE CLASSIFICATION in §3.1 and §3.2 and for FACE RECOGNITION in §3.3.

3.1 Image Classification with CIFAR-10

We first present the model quality with different decentralized learning algorithms over the IID and Non-IID settings for IMAGE CLASSIFICATION over the CIFAR-10 dataset. We use five partitions ($K = 5$) in this evaluation. As the CIFAR-10 dataset consists of ten object classes, each data partition has two object classes in the Non-IID setting. Figure 1 shows the results with four popular DNNs (AlexNet, GoogLeNet, LeNet, and ResNet). According to the hyper-parameter criteria in §2.2, we select $T_0 = 10\%$ for Gaia, $Iter_{Local} = 20$ for FederatedAveraging, and $E_{warm} = 8$ for DeepGradientCompression. We make two major observations.

1) It is a pervasive problem. All three decentralized learning algorithms lose significant model quality for *all* four DNNs in the Non-IID setting. We see that while these algorithms retain the validation accuracy of BSP in the IID setting with $15\times$ – $20\times$ communication savings (agreeing with the results from the original papers for these algorithms), they lose 3% to 74% validation accuracy in the Non-IID setting. Simply running these algorithms for more

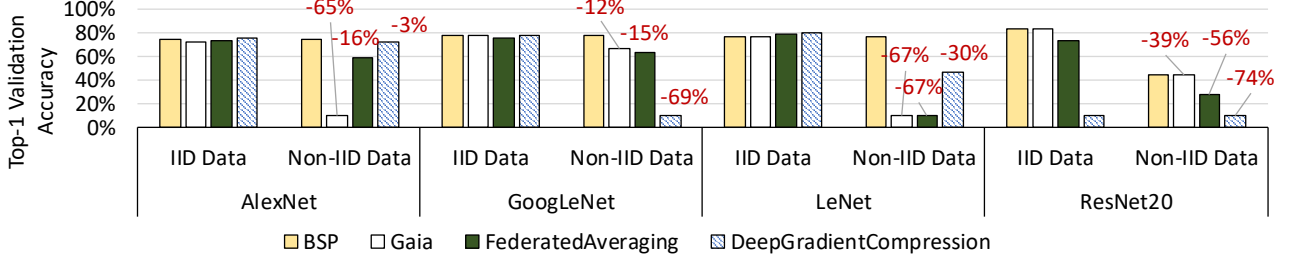


Figure 1: Top-1 validation accuracy for IMAGE CLASSIFICATION over the CIFAR-10 dataset. Each “-x%” label indicates the accuracy loss from BSP in the IID setting.

epochs would not help because the training/validation accuracy has already stopped improving. Furthermore, the training is completely diverged in some cases, such as DeepGradientCompression with GoogLeNet and ResNet20 (DeepGradientCompression with ResNet20 also diverges in the IID setting). The pervasiveness of the problem is quite surprising, as we have a diverse set of decentralized learning algorithms and DNNs. This result shows that Non-IID data is a pervasive and challenging problem for decentralized learning, and this problem has been heavily understudied. §4 discusses the cause of this problem.

2) Even BSP cannot completely solve this problem. We see that even BSP, with its full communication every iteration, cannot retain model quality for some DNNs in the Non-IID setting. In particular, the validation accuracy of ResNet20 in the Non-IID setting is 39% lower than that in the IID setting. This finding suggests that, for some DNNs, it *may not be possible* to solve the Non-IID data challenge by communicating more frequently between data partitions (P_k). We find that this problem not only exists in ResNet20, but in all DNNs we study with batch normalization layers (ResNet10, BN-LeNet (Ioffe & Szegedy, 2015) and Inception-v3 (Szegedy et al., 2016)). We discuss this problem and potential solutions in §5.

3.2 Image Classification with ImageNet

We study IMAGE CLASSIFICATION over the ImageNet dataset (Russakovsky et al., 2015) dataset (1,000 image classes) to see if the Non-IID data problem exists in different datasets. We use two partitions ($K = 2$) in this experiment so each partition gets 500 image classes. According to the hyper-parameter criteria in §2.2, we select $T_0 = 40\%$ for Gaia, $Iter_{Local} = 200$ for FederatedAveraging, and $E_{warm} = 4$ for DeepGradientCompression.

The same trend in different datasets. Figure 2 illustrates the validation accuracy in the IID and Non-IID settings. Interestingly, we observe the same problems in the ImageNet dataset, whose number of classes is two orders of magnitude more than the CIFAR-10 dataset. First, we see that Gaia and FederatedAveraging lose significant validation accuracy (8.1% to 27.2%) for both DNNs in the Non-IID setting. On the other hand, while DeepGradientCompression is able to retain the validation accuracy for GoogLeNet in the Non-IID

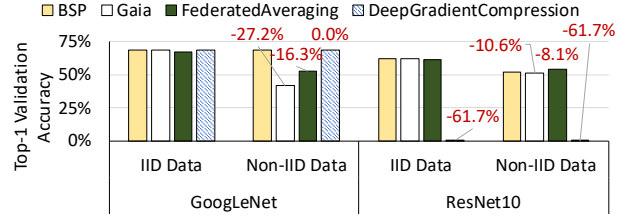


Figure 2: Top-1 validation accuracy for IMAGE CLASSIFICATION over the ImageNet dataset. Each “-x%” label indicates the accuracy loss from BSP in the IID setting.

setting, it cannot converge to a useful model for ResNet10. Second, BSP also cannot retain the validation accuracy for ResNet10 in the Non-IID setting, which concurs with our observation in the CIFAR-10 study. These results show that the Non-IID data problem not only exists in various decentralized learning algorithms and DNNs, but also exists in different datasets.

3.3 Face Recognition

We further examine another popular ML application, FACE RECOGNITION, to see if the Non-IID data problem is a fundamental challenge across different applications. We again use two partitions ($K = 2$) in this evaluation, and we store different people’s faces in different partitions in the Non-IID setting. According to the hyper-parameter criteria in §2.2, we select $T_0 = 20\%$ for Gaia, $Iter_{Local} = 50$ for FederatedAveraging, and $E_{warm} = 8$ for DeepGradientCompression. It is worth noting that the verification process of FACE RECOGNITION is fundamentally different from IMAGE CLASSIFICATION, as FACE RECOGNITION does *not* use the classification layer (and thus the training labels) at all in the verification process. Instead, for each pair of verification images, the trained DNN is used to compute a feature vector for each image, and the distance between these feature vectors is used to determine if the two images belong to the same person.

The same problem in different applications. Figure 3 presents the LFW verification accuracy using different decentralized learning algorithms in the IID and Non-IID settings. Again, the same problem happens in this application: these decentralized learning algorithms work well in the IID

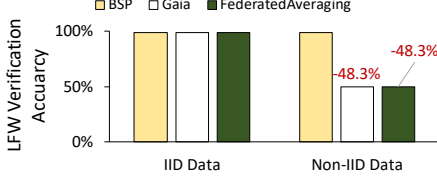


Figure 3: LFW verification accuracy for FACE RECOGNITION. Each “-x%” label indicates the accuracy loss from BSP in the IID setting.

setting, but they lose significant accuracy in the Non-IID setting. In fact, both Gaia and FederatedAveraging cannot converge to a useful model in the Non-IID setting, and their 50% accuracy is from random guessing (the verification process is a series of binary questions). This result is particularly noteworthy as FACE RECOGNITION uses a vastly different verification process that does not rely on the training labels, which are used to create the Non-IID setting to begin with. We conclude that Non-IID data is a fundamental and pervasive problem across various applications, datasets, models, and decentralized learning algorithms.

4 PROBLEMS OF DECENTRALIZED LEARNING ALGORITHMS

The results in §3 show that three diverse decentralized learning algorithms all suffer drastic accuracy loss in the Non-IID setting. We investigate the potential reasons for this (§4.1) and the sensitivity to hyper-parameter choice (§4.2).

4.1 Reasons for Model Quality Loss

Gaia. We extract the Gaia-trained models from both partitions (denoted DC-0 and DC-1) for IMAGE CLASSIFICATION over the ImageNet dataset, and then evaluate the validation accuracy of each model based on the *image classes* in each partition. As Figure 4 shows, the validation accuracy is pretty consistent among the two sets of image classes when training the model in the IID setting: the results for IID DC-0 Model are shown, and IID DC-1 Model is the same. However, the validation accuracy varies drastically under the Non-IID setting (Non-IID DC-0 Model and Non-IID DC-1 Model). Specifically, both models perform well for the image classes in their respective partition, but they perform very poorly for the image classes that are *not* in their respective partition. This reveals that using Gaia in the Non-IID setting results in *completely different* models among data partitions, and each model is only good for recognizing the image classes in its data partition.

This raises the following question: How does Gaia produce completely different models in the Non-IID setting, given that Gaia synchronizes all significant updates (Δw_j) to ensure that the differences across models in each weight w_j is insignificant (§2)? To answer this, we first compare each weight w_j in the Non-IID DC-0 and DC-1 Models, and find that the average difference among all the weights is only

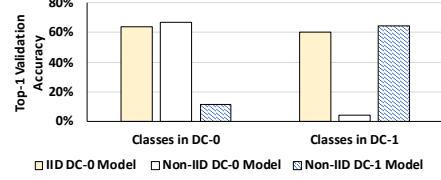


Figure 4: Top-1 validation accuracy (ImageNet) for models in different partitions.

0.5% (reflecting that the threshold for significance in the last epoch was 1%). However, we find that given the same input image, the *neuron* values are vastly different (at an average difference of 173%). This finding suggests that small model differences can result in completely different models. Mathematically, this is because weights are both positive and negative: a small percentage difference in individual weights of a neuron can lead to a large percentage difference in its value. As Gaia eliminates insignificant communication, it creates an opportunity for models in each data partition to specialize for the image classes in their respective data partition, at the expense of other classes.

DeepGradientCompression. While local model specialization explains why Gaia performs poorly in the Non-IID setting, it is still unclear why other decentralized learning algorithms also exhibit the same problem. More specifically, DeepGradientCompression and FederatedAveraging always maintain *one* global model, hence there is no room for local model specialization. To understand why these algorithms perform poorly, we study the average residual update delta ($||\Delta w_i/w_i||$) with DeepGradientCompression. This number represents the magnitude of the gradients that have *not* yet been exchanged among different P_k , due to its communicating only a fixed number of gradients in each epoch (§2). Thus, it can be seen as the amount of gradient divergence among different P_k .

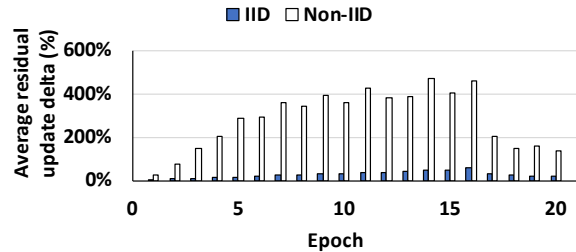


Figure 5: Average residual update delta (%) for DeepGradientCompression over the first 20 epochs.

Figure 5 depicts the average residual update delta for the first 20 training epochs when training ResNet20 over the CIFAR-10 dataset. We show only the first 20 epochs because the training diverges after that in the Non-IID setting. As the figure shows, the average residual update delta is an order of magnitude higher in the Non-IID setting (283%) than that in the IID setting (27%). Hence, each P_k generates large gradients in the Non-IID setting, which is not

surprising as each P_k sees vastly different training data in the Non-IID setting. However, these large gradients are not synchronized because DeepGradientCompression sparsifies the gradients at a fixed rate. When they are finally synchronized, they may have diverged so much from the global model that they lead to the divergence of the whole model. Our experiments also support this proposition, as we see DeepGradientCompression diverges much more often in the Non-IID setting.

FederatedAveraging. The above analysis for DeepGradientCompression can also apply to FederatedAveraging, which delays communication from each P_k by a fixed number of local iterations. If the weights in different P_k diverge too much, the synchronized global model can lose accuracy or completely diverge (Zhao et al., 2018). We validate this by plotting the average local weight update delta for FederatedAveraging at each global synchronization ($||\Delta w_i/w_i||$, where w_i is the averaged global model weight). Figure 6 depicts this number for the first 25 training epochs when training AlexNet over the CIFAR-10 dataset. As the figure shows, the average local weight update delta in the Non-IID setting (48.5%) is much higher than that in the IID setting (20.2%), which explains why Non-IID data partitions lead to major accuracy loss for FederatedAveraging. The difference is less pronounced than with DeepGradientCompression, so the impact on accuracy is smaller.

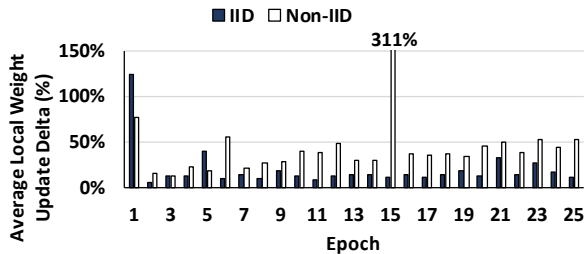


Figure 6: Average local update delta (%) for FederatedAveraging over the first 25 epochs.

4.2 Algorithm Hyper-Parameters

We now study the sensitivity of the non-IID problem to hyper-parameter choice. Table 1 presents the Gaia results for varying its T_0 hyper-parameter (§2.2) when training on CIFAR-10, and we leave the results for the other two algorithms and more models to Appendix C. As the table shows, we study seven choices for T_0 and compare the results with BSP. We make two main observations.

First, almost all hyper-parameter settings lose significant accuracy in the Non-IID setting (relative to BSP in the IID setting). Even with a relatively conservative hyper-parameter setting (e.g., $T_0 = 2\%$, the most communication-intensive of the choices shown), we still see a 3.3% and 21.9% ac-

curacy loss. On the other hand, the exact same hyper-parameter choice for Gaia in the IID setting can achieve close to BSP-level accuracy (within 1.1%). We see the same trend with much more aggressive hyper-parameter settings as well (e.g., $T_0 = 40\%$). This shows that the problem of Non-IID data partitions is not specific to particular hyper-parameter settings, and that hyper-parameter settings that work well in the IID setting may perform poorly in the Non-IID setting.

Second, more conservative hyper-parameter settings (which implies more frequent communication among the P_k) often greatly decrease the accuracy loss in the Non-IID setting. For example, the validation accuracy with $T_0 = 2\%$ is significantly higher than the one with $T_0 = 30\%$. This suggests that we may be able to use more frequent communication among the P_k for higher model quality in the Non-IID setting (mitigating the “tug-of-war” among the P_k (§2.1)).

Configuration	AlexNet		GoogLeNet	
	IID	Non-IID	IID	Non-IID
BSP	74.9%	75.0%	79.1%	78.9%
$T_0 = 2\%$	73.8%	70.5%	78.4%	56.5%
$T_0 = 5\%$	73.2%	71.4%	77.6%	75.6%
$T_0 = 10\%$	73.0%	10.0%	78.4%	68.0%
$T_0 = 20\%$	72.5%	37.6%	77.7%	67.0%
$T_0 = 30\%$	72.4%	26.0%	77.5%	23.9%
$T_0 = 40\%$	71.4%	20.1%	77.2%	33.4%
$T_0 = 50\%$	10.0%	22.2%	76.2%	26.7%

Table 1: Top-1 validation accuracy (CIFAR-10) varying Gaia’s T_0 parameter. Configurations with more than 2% accuracy loss from BSP in the IID setting are highlighted.

5 BATCH NORMALIZATION: PROBLEM AND SOLUTION

As §3 discusses, even BSP cannot retain model quality in the Non-IID setting for DNNs with batch normalization layers. In this section, we first discuss why batch normalization is particularly vulnerable in the Non-IID setting (§5.1) and then study alternative normalization techniques, including one—Group Normalization—that works better in this setting (§5.2).

5.1 The Problem of Batch Normalization in the Non-IID Setting

Batch normalization (Ioffe & Szegedy, 2015) (BatchNorm) is one of the most popular mechanisms in deep learning, and it has been employed by default in most deep learning models (more than 11,000 citations). BatchNorm enables faster and more stable DNN training because it enables larger learning rates, which in turn make convergence much faster and help avoid sharp local minimum (hence, the model

generalizes better).

How BatchNorm works. BatchNorm aims to stabilize a DNN by normalizing the input distribution of selected layers such that the inputs x_i on each channel i of the layer have zero mean ($\mu_{x_i} = 0$) and unit variance ($\sigma_{x_i} = 1$). Because the global mean and variance is unattainable with stochastic training, BatchNorm uses *minibatch mean and variance* as an estimate of the global mean and variance. Specifically, for each minibatch \mathcal{B} , BatchNorm calculates the minibatch mean $\mu_{\mathcal{B}}$ and variance $\sigma_{\mathcal{B}}$, and then uses $\mu_{\mathcal{B}}$ and $\sigma_{\mathcal{B}}$ to normalize each x_i in \mathcal{B} (Ioffe & Szegedy, 2015). Recent work shows that BatchNorm enables larger learning rates because: (i) BatchNorm corrects large gradient updates that could result in divergence (Bjorck et al., 2018) and (ii) BatchNorm makes the underlying problem’s landscape significantly more smooth (Santurkar et al., 2018).

BatchNorm and the Non-IID setting. While BatchNorm is effective in practice, its dependence on minibatch mean and variance ($\mu_{\mathcal{B}}$ and $\sigma_{\mathcal{B}}$) is known to be problematic in certain settings. This is because BatchNorm uses $\mu_{\mathcal{B}}$ and $\sigma_{\mathcal{B}}$ for training, but it typically uses an estimated global mean and variance (μ and σ) for validation. If there is a major mismatch between these means and variances, the validation accuracy is going to be low because the input distribution during validation does not match the distribution during training. This can happen if the minibatch size is small or the sampling of minibatches is not IID (Ioffe, 2017). The Non-IID setting in our study exacerbates this problem because each data partition P_k sees very different training samples. Hence, the $\mu_{\mathcal{B}}$ and $\sigma_{\mathcal{B}}$ in each P_k can vary significantly in the Non-IID setting, and the synchronized global model may not work for *any* set of data. Worse still, we cannot simply increase the minibatch size or do better minibatch sampling to solve this problem, because in the Non-IID setting the underlying training dataset in each P_k does not represent the global training dataset.

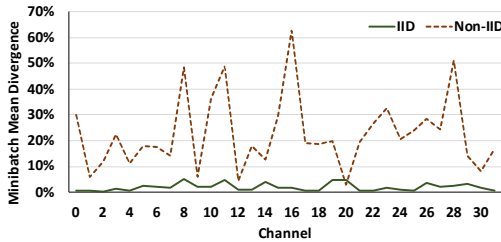


Figure 7: Minibatch mean divergence for the first layer of BN-LeNet over CIFAR-10 using two P_k .

We validate if there is indeed major divergence in $\mu_{\mathcal{B}}$ and $\sigma_{\mathcal{B}}$ among different P_k in the Non-IID setting. We calculate the divergence of $\mu_{\mathcal{B}}$ as the difference between $\mu_{\mathcal{B}}$ in different P_k over the average $\mu_{\mathcal{B}}$ (i.e., it is $\frac{\|\mu_{\mathcal{B}, P_0} - \mu_{\mathcal{B}, P_1}\|}{\|AVG(\mu_{\mathcal{B}, P_0}, \mu_{\mathcal{B}, P_1})\|}$ for two partitions P_0 and P_1). We use the average $\mu_{\mathcal{B}}$ over every 100 minibatches in each P_k so that we get better

estimation. Figure 7 depicts the divergence of $\mu_{\mathcal{B}}$ for each channel of the first layer of BN-LeNet, which is constructed by inserting BatchNorm to LeNet after each convolutional layer. As we see, the divergence of $\mu_{\mathcal{B}}$ is significantly larger in the Non-IID setting (between 6% to 51%) than that in the IID setting (between 1% to 5%). We also observe the same trend in minibatch variances $\sigma_{\mathcal{B}}$ (not shown). As discussed earlier, this phenomenon is detrimental to training: Each P_k uses very different $\mu_{\mathcal{B}}$ and $\sigma_{\mathcal{B}}$ to normalize its model, but the resultant global model can use only one μ and σ which cannot match all of these diverse batch means and variances. As this problem has nothing to do with the frequency of communication among P_k , it explains why even BSP cannot retain model accuracy for BatchNorm in the Non-IID setting.

5.2 Alternatives to Batch Normalization

As the problem of BatchNorm in the Non-IID setting is due to its dependence on minibatches, the natural solution is to replace BatchNorm with alternative normalization mechanisms that are *not* dependent on minibatches. Unfortunately, most existing alternative normalization mechanisms have their own drawbacks. We first discuss the normalization mechanisms that have major shortcomings, and then we discuss a particular mechanism that may be used instead.

Weight Normalization (Salimans & Kingma, 2016).

Weight Normalization (WeightNorm) is a normalization scheme that normalizes the weights in a DNN as oppose to the neurons (which is what BatchNorm and most other normalization techniques do). WeightNorm is not dependent on minibatches as it is normalizing the weights. However, while WeightNorm can effectively control the variance of the neurons, it still needs a mean-only BatchNorm in many cases to achieve the model quality and training speeds of BatchNorm (Salimans & Kingma, 2016). This mean-only BatchNorm makes WeightNorm vulnerable to the Non-IID setting again, because there is a large divergence in $\mu_{\mathcal{B}}$ among the P_k in the Non-IID setting (§5.1).

Layer Normalization (Ba et al., 2016).

Layer Normalization (LayerNorm) is a technique that is inspired by BatchNorm. Instead of computing the mean and variance of a minibatch for each *channel*, LayerNorm computes the mean and variance across all channels for each *sample*. Specifically, if the inputs are four-dimensional vectors $\mathcal{B} \times \mathcal{C} \times \mathcal{W} \times \mathcal{H}$ (batch \times channel \times width \times height), BatchNorm produces \mathcal{C} means and variances along the $\mathcal{B} \times \mathcal{W} \times \mathcal{H}$ dimensions. On the other hand, LayerNorm produces \mathcal{B} means and variances along the $\mathcal{C} \times \mathcal{W} \times \mathcal{H}$ dimensions (per-sample mean and variance). As the normalization is done on a per-sample basis, LayerNorm is not dependent on minibatches. However, LayerNorm makes a key assumption that all inputs make similar contributions to the final prediction. But this assumption does not hold for some models such as convolutional neural networks, where the activation of

neurons should not be normalized with non-activated neurons. As a result, BatchNorm still outperforms LayerNorm for these models (Ba et al., 2016).

Batch Renormalization (Ioffe, 2017). Batch Renormalization (BatchReNorm) is an extension to BatchNorm that aims to alleviate the problem of small minibatches (or inaccurate minibatch mean, μ_B , and variance, σ_B). BatchReNorm achieves this by incorporating the estimated global mean (μ) and variance (σ) during *training*, and introducing two hyper-parameters to contain the difference between (μ_B, σ_B) and (μ, σ) . These two hyper-parameters are gradually relaxed such that the earlier training phase is more like BatchNorm, and the later phase is more like BatchReNorm.

We evaluate BatchReNorm with BN-LeNet over CIFAR-10 to see if BatchReNorm can solve the problem of Non-IID data partitions. We replace all BatchNorm layers with BatchReNorm layers, and we carefully select the BatchReNorm hyper-parameters so that BatchReNorm achieves the highest validation accuracy in both the IID and Non-IID settings. Table 2 shows the Top-1 validation accuracy. We see that while BatchNorm and BatchReNorm achieve similar accuracy in the IID setting, they both perform worse in the Non-IID setting. In particular, while BatchReNorm performs much better than BatchNorm in the Non-IID setting (75.3% vs. 65.4%), BatchReNorm still loses $\sim 3\%$ accuracy compared to the IID setting. This is not surprising, because BatchReNorm still relies on minibatches to certain degree, and prior work has shown that BatchReNorm’s performance still degrades when the mini-batch size is small (Ioffe, 2017). Hence, BatchReNorm cannot completely solve the problem of Non-IID data partitions, which is a more challenging problem than small minibatches.

BatchNorm		BatchReNorm	
IID	Non-IID	IID	Non-IID
78.8%	65.4%	78.1%	75.3%

Table 2: Top-1 validation accuracy (CIFAR-10) with BatchNorm and BatchReNorm for BN-LeNet, using BSP with $K = 2$ partitions.

Group Normalization (Wu & He, 2018). Group Normalization (GroupNorm) is an alternative normalization mechanism that aims to overcome the shortcomings of BatchNorm and LayerNorm. GroupNorm divides adjacent channels into groups of a prespecified size \mathcal{G}_{size} , and computes the per-group mean and variance for *each* input sample. Specifically, for a four-dimensional input $\mathcal{B} \times \mathcal{C} \times \mathcal{W} \times \mathcal{H}$, GroupNorm partitions the set of channels (\mathcal{C}) into multiple groups (\mathcal{G}) of size \mathcal{G}_{size} . GroupNorm then computes $|\mathcal{B}| \cdot |\mathcal{G}|$ means and variances along the $\mathcal{G}_{size} \times \mathcal{W} \times \mathcal{H}$ dimension. Hence, GroupNorm does not depend on minibatches for normal-

ization (the shortcoming of BatchNorm), and GroupNorm does not assume all channels make equal contributions (the shortcoming of LayerNorm).

We evaluate GroupNorm with BN-LeNet over CIFAR-10 to see if we can use GroupNorm as an alternative to BatchNorm in the Non-IID setting. We carefully select $\mathcal{G}_{size} = 2$, which works best with this DNN. Figure 8 shows the Top-1 validation accuracy with GroupNorm and BatchNorm across decentralized learning algorithms. We make two main observations.

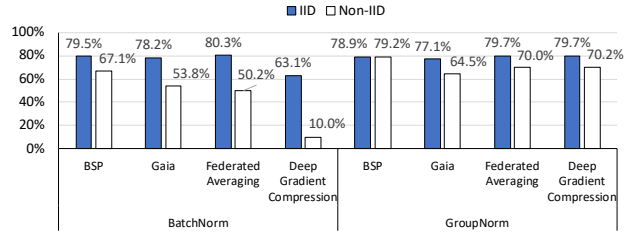


Figure 8: Top-1 validation accuracy (CIFAR-10) with BatchNorm and GroupNorm for BN-LeNet with $K = 5$ partitions.

First, GroupNorm successfully recovers the accuracy loss of BatchNorm with BSP in the Non-IID setting. As the figure shows, GroupNorm with BSP achieves 79.2% validation accuracy in the Non-IID setting, which is as good as the accuracy in the IID setting. This shows GroupNorm can be used as an alternative to BatchNorm to overcome the Non-IID data challenge for BSP. Second, GroupNorm dramatically helps the decentralized learning algorithms to improve model accuracy in the Non-IID setting as well. We see that with GroupNorm, there is 14.4%, 8.9% and 8.7% accuracy loss for Gaia, FederatedAveraging and Deep-GradientCompression, respectively. While the accuracy losses are still significant, they are better than their BatchNorm counterparts by an additive 10.7%, 19.8% and 60.2%, respectively.

Summary. Overall, our study shows that GroupNorm (Wu & He, 2018) can be a good alternative to BatchNorm in the Non-IID setting, especially for computer vision tasks. For BSP, it fixes the problem, while for decentralized learning algorithms, it greatly decreases the accuracy loss. However, it is worth noting that BatchNorm is widely adopted in many DNNs, hence, more study should be done to see if GroupNorm can always replace BatchNorm for different applications and DNN models. As for other tasks such as recurrent (e.g., LSTM (Hochreiter & Schmidhuber, 1997)) and generative (e.g., GAN (Goodfellow et al., 2014)) models, other normalization techniques such as LayerNorm (Ba et al., 2016) can be good options because (i) they are shown to be effective in these tasks and (ii) they are not dependent on minibatches, hence, they are unlikely to suffer the problems of BatchNorm in the Non-IID setting.

6 DEGREE OF DEVIATION FROM IID

Our study in previous sections (§3–§5) assumes a strict case of non-IID data partitions, where each training label only exists in a data partition *exclusively*. While this assumption may be a reasonable approximation for some applications (e.g., for FACE RECOGNITION, a person’s face image may exist only in a data partition for a geo-region in which the person lives), it could be an extreme case for other applications (e.g., IMAGE CLASSIFICATION). Here, we study how the problem of non-IID data changes with the degree of deviation from IID (the skewness) by controlling the fraction of data that are non-IID (§2.2). Figure 9 illustrates the CIFAR-10 Top-1 validation accuracy of AlexNet and GN-LeNet (our name for BN-LeNet with GroupNorm replacing BatchNorm, Figure 8) in the 20%, 40%, 60% and 80% non-IID setting. We make two main observations.

1) Partial non-IID data is also problematic. We see that for all three decentralized learning algorithms, partial non-IID data still cause major accuracy loss. Even with a small degree of non-IID data such as 20%, we still see 5.8% and 3.4% accuracy loss for Gaia and FederatedAveraging in AlexNet (Figure 9a). The only exception is AlexNet with DeepGradientCompression, which retains model accuracy in partial non-IID settings. However, the same technique suffers significant accuracy loss for GN-LeNet in partial non-IID settings (Figure 9b). We conclude that the problem of non-IID data does not occur only with exclusive non-IID data partitioning, and hence, the problem exists in a vast majority of practical decentralized settings.

2) The degree of deviation from IID often determines the difficulty level of the problem. We observe that the degree of skew changes the landscape of the problem significantly. In most cases, the model accuracy gets worse with higher degrees of skew, and the accuracy gap between 80% and 20% non-IID data can be as large as 7.4% (GN-LeNet with DeepGradientCompression). We see that while most decentralized learning algorithms can retain model quality within certain degrees of skew, there is usually a limit. For example, when training over 20% non-IID data, all three decentralized learning algorithms stay within 1.3% accuracy loss for GN-LeNet (Figure 9b). However, their accuracy losses become unacceptable when they are dealing with 40% or higher non-IID data.

7 OUR APPROACH: SkewScout

To address the problem of non-IID data partitions, we introduce SkewScout, a generic, system-level approach that enables communication-efficient decentralized learning over *arbitrarily* non-IID data partitions. We provide an overview of SkewScout (§7.1), describe its key mechanisms (§7.2), and present evaluation results (§7.3).

7.1 Overview of SkewScout

The goal of SkewScout is a system-level solution that (i) enables high-accuracy, communication-efficient decentralized learning over arbitrarily non-IID data partitions; and (ii) is general enough to be applicable to a wide range of ML applications, ML systems, and decentralized learning algorithms. To this end, we design SkewScout as a system-level module that can be integrated with various decentralized learning algorithms and ML systems.

Figure 10 overviews the SkewScout design.

- **Estimate the degree of deviation from IID.** As §6 shows, knowing the degree of skew is very useful to determine an appropriate solution. To learn this key information, SkewScout periodically moves the ML model from one data partition (P_k) to another during training (*model traveling*, ❶ in Figure 10). SkewScout then evaluates how well a model performs on a remote data partition by evaluating the model accuracy with a subset of training data on the remote node. As we already know the training accuracy of this model in its originated data partition, we can infer the *accuracy loss* in this remote data partition (❷). The accuracy loss is essentially the performance gap for the same model over two different data partitions, which can be used as an approximation of the degree of skew. For example, it is very likely that a remote data partition consists of very different data characteristics if the model in the local data partition has reached training accuracy 60%, but the same model achieves only 30% accuracy in the remote data partition. More importantly, accuracy loss *directly* captures the extent to which the model underperforms on the different data partition.
- **Adaptive communication control (❸).** Based on the accuracy loss SkewScout learns from model traveling, SkewScout controls the tightness of communication among data partitions to retain model quality. SkewScout controls the communication tightness by automatically tuning the hyper-parameters of the decentralized learning algorithm (§4.2). This tuning process is essentially solving an optimization problem that aims to minimize communication among data partitions while keeping accuracy loss within a reasonable threshold (§7.2 provides further details).

SkewScout handles non-IID data partitions in a manner that is transparent to ML applications and decentralized learning algorithms, and it controls communication based on the accuracy loss across partitions. Thus, we do not need to use the most conservative mechanism (e.g., BSP) all the time, and can adapt to whatever skew is present for the particular ML application and its training data partitions (§6).

7.2 Mechanism Details

We now discuss the mechanisms of SkewScout in detail.

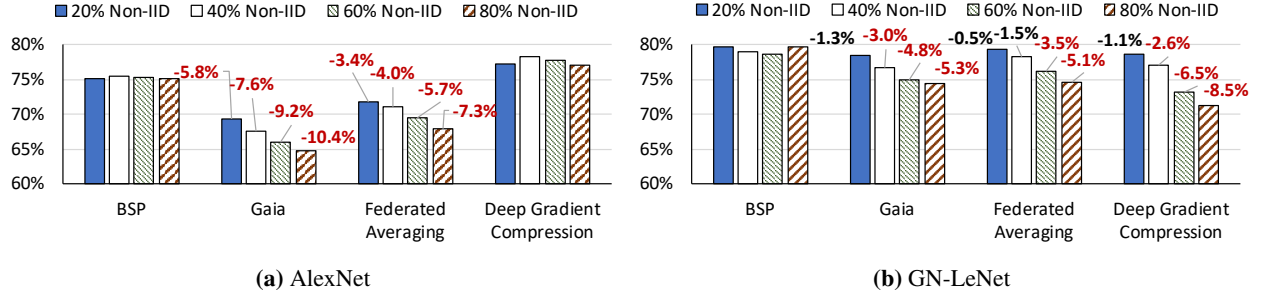


Figure 9: Top-1 validation accuracy (CIFAR-10) over various degrees of non-IID data. We have zoomed in on 60% accuracy and above. The “-x%” label on each bar indicates the accuracy loss from BSP in the IID setting.

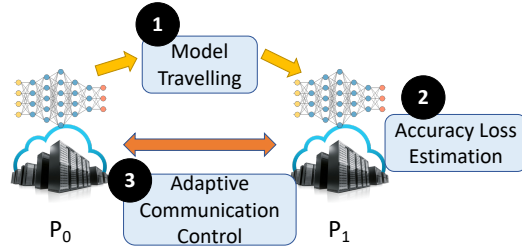


Figure 10: Overview of SkewScout

Accuracy Loss. The accuracy loss between data partitions represents the degree of model divergence. As §4.1 discusses, ML models in different data partitions tend to specialize for their training data, especially when we use decentralized learning algorithms to relax communication.

Figure 11 demonstrates the above observation by plotting the accuracy loss between different data partitions when training GoogleNet over CIFAR-10 with Gaia. Two observations are in order. First, the accuracy loss changes drastically from the IID setting (0.4% on average) to the Non-IID setting (39.6% on average). This is expected as each data partition sees very different training data in the Non-IID setting, which leads to very different models in different data partitions. Second, more conservative hyper-parameters can lead to smaller accuracy drop in the Non-IID setting. For example, the accuracy loss for $T_0 = 2\%$ is significantly smaller than for larger settings of T_0 .

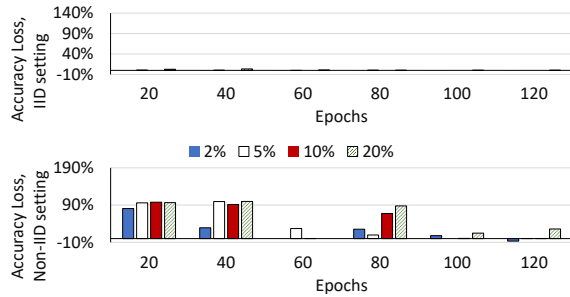


Figure 11: Training accuracy loss between data partitions when training GoogleNet over CIFAR-10 with Gaia. Each bar represents a T_0 for Gaia.

Based on the above observation, we can use accuracy loss (i) to estimate how much the models diverge from each other (reflecting training data differences); and (ii) to serve as an objective function for communication control. With accuracy loss, we do not need any domain-specific information from each ML application to learn and adapt to different degrees of deviation from IID, which makes SkewScout much more widely applicable.

Communication Control. The goal of communication control is to retain model quality while minimizing communication among data partitions. Specifically, given a set of hyper-parameters θ_t for each iteration (or minibatch) t , the optimization problem for SkewScout is to minimize the total amount of communication for a data partition P_k :

$$\operatorname{argmin}_{\theta, MTP} \left(\sum_{mt=0}^{\lceil \frac{T(\theta)}{MTP} \rceil} \sum_{t=mt \cdot MTP}^{(mt+1) \cdot MTP} C(\theta_t) + \sum_{mt=0}^{\lceil \frac{T(\theta)}{MTP} \rceil} CM \right) \quad (1)$$

where $T(\theta)$ is the total number of iterations to achieve the target model accuracy given all hyper-parameters θ throughout the training, $C(\theta_t)$ is the amount of communication given θ_t , MTP is the period size (in iterations) for model traveling, and CM is the communication cost for the ML model (for model traveling).

In practice, however, it is impossible to optimize for Equation 1 with one-pass training because we cannot know $T(\theta)$ with different θ unless we train the model multiple times. We solve this problem by optimizing a proxy problem, which aims to minimize the communication while keeping the *accuracy loss* to a small threshold σ_{AL} so that we can control model divergence caused by non-IID data partitions. Specifically, our target function is:

$$\operatorname{argmin}_{\theta_t} \left(\lambda_{AL} (\max(0, AL(\theta_t) - \sigma_{AL})) + \lambda_C \frac{C(\theta_t)}{CM} \right) \quad (2)$$

where $AL(\theta_t)$ is the accuracy loss based on the previously selected hyper-parameter (we memoize the most recent value for each θ), and λ_{AL} , λ_C are given parameters to determine the weight of accuracy loss and communication,

respectively. We can employ various auto-tuning algorithms with Equation 2 to select θ_t such as hill climbing, stochastic hill climbing (Russell & Norvig, 2016), and simulated annealing (Van Laarhoven & Aarts, 1987). Note that we make *MTP* not tunable here to further simplify the tuning.

Model Traveling Overhead. Using model traveling to learn accuracy loss can lead to heavy communication overhead if we need to do so for *each pair* of data partitions, especially if we have a large number of data partitions. For broadcast-based decentralized learning settings (e.g., geo-distributed learning), we leverage an overlay network to reduce the communication overhead for model traveling. Specifically, we use hubs to combine and broadcast models (Hsieh et al., 2017). The extra hops incurred are fine because model traveling is not latency sensitive. As for server-client decentralized learning settings (e.g., federated learning), SkewScout only needs to control the communication frequency between server and clients, and the overhead of model traveling can be combined with model downloading at the beginning of each communication round between the server and clients.

7.3 Evaluation Results

We implement and evaluate SkewScout in a GPU parameter server system (Cui et al., 2016) based on Caffe (Jia et al., 2014). We evaluate several aforementioned auto-tuning algorithms and we find that hill climbing provides the best results. We compare SkewScout with two other baselines: (1) BSP: the most communication-heavy approach that retains model quality in all Non-IID settings; and (2) Oracle: the ideal, yet unrealistic, approach that selects the most communication-efficient θ that retains model quality by *running all possible* θ in each setting prior to measured execution. Figure 12 shows the communication savings over BSP for both SkewScout and Oracle when training with Gaia. Note that all results achieve the same validation accuracy as BSP. We make two main observations.

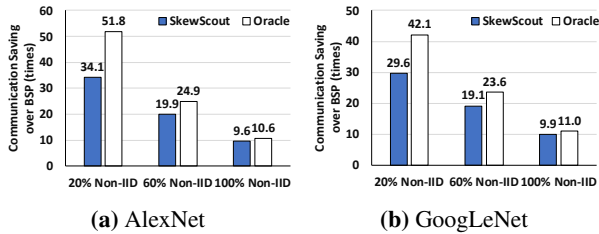


Figure 12: Communication savings over BSP with SkewScout and Oracle for training over CIFAR-10.

First, SkewScout is much more effective than BSP in handling Non-IID settings. Overall, SkewScout achieves 9.6–34.1 \times communication savings over BSP in various Non-IID settings without sacrificing model accuracy. As expected, SkewScout saves more communication with less skewed data because SkewScout can loosen communication in these

settings (§6).

Second, SkewScout is not far from the ideal Oracle baseline. Overall, SkewScout requires only 1.1–1.5 \times more communication than Oracle to achieve the same model accuracy. SkewScout cannot match the communication savings of Oracle because: (i) SkewScout needs to do model traveling periodically, which leads to some extra overheads; and (ii) for some θ , high accuracy loss at the beginning can still end up with a high quality model, which SkewScout cannot foresee. As Oracle requires many runs in practice, we conclude that SkewScout is an effective, one-pass solution for decentralized learning over non-IID data partitions.

8 RELATED WORK

To our knowledge, this is the first detailed study on the problem of non-IID data partitions for decentralized learning. Our study shows that this is a fundamental and pervasive problem, and we investigate various aspects of this problem, such as decentralized learning algorithms, batch normalization, and the degree of non-IID data, as well as present our SkewScout approach. Here, we discuss related work.

Large-scale systems for centralized learning. There are many large-scale ML systems that aim to enable efficient ML training with *centralized* datasets (e.g., (Recht et al., 2011; Low et al., 2012; Chilimbi et al., 2014; Dean et al., 2012; Ho et al., 2013; Cui et al., 2014; Li et al., 2014a; Chen et al., 2015; Goyal et al., 2017)), where the data reside within a single data center. Some of them propose communication-efficient designs, such as relaxing synchronization requirements (Recht et al., 2011; Ho et al., 2013; Goyal et al., 2017) or sending fewer updates to parameter servers (Li et al., 2014a;b). These works assume the training data are centralized so they can be easily partitioned among the machines performing the training in an IID manner (e.g., by random shuffling). Hence, they are neither designed nor validated on non-IID data partitions.

Communication-efficient training for specific algorithms. A large body of prior work proposes ML training algorithms to reduce the dependency on intensive parameter updates to enable more efficient parallel training (e.g., (Jaggi et al., 2014; Zhang et al., 2013; Zinkevich et al., 2010; Takác et al., 2013; Neiswanger et al., 2014; Shamir et al., 2014; Zhang & Lin, 2015; Shalev-Shwartz & Zhang, 2013)). These works reduce communication overhead by proposing algorithm-specific approaches, such as solving a dual problem (Shalev-Shwartz & Zhang, 2013; Takác et al., 2013; Jaggi et al., 2014) or employing a different optimization algorithm (Rakhlin et al., 2012; Zhang & Lin, 2015). The main drawback of these approaches is that they are not general and their applicability depends on the ML application. Besides, these works also assume centralized, IID data partitions. Thus, their effectiveness over decentralized, non-IID data partitions needs much more study.

Decentralized learning. As most training data are generated in a decentralized manner, prior work proposes communication-efficient algorithms (e.g., (Hsieh et al., 2017; McMahan et al., 2017; Shokri & Shmatikov, 2015; Lin et al., 2018; Tang et al., 2018)) for ML training over decentralized datasets. However, the major focus of these works is to reduce communication overhead among data partitions, and they either (i) assume the data partitions are IID (Hsieh et al., 2017; Shokri & Shmatikov, 2015; Lin et al., 2018) or (ii) conduct only a limited study on non-IID data partitions (McMahan et al., 2017; Tang et al., 2018). As our study shows, these decentralized learning algorithms lose significant model quality in the Non-IID setting (§3). Some recent work (Zhao et al., 2018; Smith et al., 2017) investigates the problem of non-IID data partitions. For example, instead of training a global model to fit non-IID data partitions, federated multi-task learning (Smith et al., 2017) proposes training local models for each data partition while leveraging other data partitions to improve the model accuracy. However, this approach does not solve the problem for global models, which are essential when a local model is unavailable (e.g., a brand new partition without training data) or ineffective (e.g., a partition with too few training examples for a class). The closest to our work is Zhao et al.’s study (Zhao et al., 2018) on FederatedAveraging over non-IID data, which shows FederatedAveraging suffers significant accuracy loss in the Non-IID setting. While the result of their study aligns with our observations on FederatedAveraging, our study (i) broadens the problem scope to a variety of decentralized learning algorithms, ML applications, DNN models, and datasets, (ii) explores the problem of batch normalization and possible solutions, and (iii) designs and evaluates SkewScout.

9 DISCUSSION: REGIMES OF NON-IID DATA

Our study has focused on *label-based* partitioning of data, in which the distribution of labels varies across partitions. In this section, we present a broader taxonomy of regimes of non-IID data, as well as various possible strategies for dealing with non-IID data, the study of which are left to future work. We assume a general setting in which there may be many disjoint partitions, with each partition holding data collected from devices (mobile phones, video cameras, etc.) from a particular geographic region and time window.

Violations of Independence. Common ways in which data tend to deviate from being independently drawn from an overall distribution are:

- *Intra-partition correlation:* If the data within a partition are processed in an insufficiently-random order, e.g., ordered by collection device and/or by time, then independence is violated. For example, consecutive frames in a video are highly correlated, even if the camera is

moving.

- *Inter-partition correlation:* Devices sharing a common feature can have correlated data across partitions. For example, neighboring geo-locations have the same diurnal effects (daylight, workday patterns), have correlated weather patterns (major storms), and can witness the same phenomena (eclipses).

Violations of Identicalness. Common ways in which data tend to deviate from being identically distributed are:

- *Quantity skew:* Different partitions can hold vastly different amounts of data. For example, some partitions may collect data from fewer devices or from devices that produce less data.
- *Label distribution skew:* Because partitions are tied to particular geo-regions, the distribution of labels varies across partitions. For example, kangaroos are only in Australia or zoos, and a person’s face is only in a few locations worldwide. The study in this paper focused on this setting.
- *Same label, different features:* The same label can have very different “feature vectors” in different partitions, e.g., due to cultural differences, weather effects, standards of living, etc. For example, images of homes can vary dramatically around the world and items of clothing vary widely. Even within the U.S., images of parked cars in the winter will be snow-covered only in certain parts of the country. The same label can also look very different at different times, at different time scales: day vs. night, seasonal effects, natural disasters, fashion and design trends, etc.
- *Same features, different label:* Because of personal preferences, the same feature vectors in a training data item can have different labels. For example, labels that reflect sentiment or next word predictors have personal/regional biases.

As noted in some of the above examples, non-IID-ness can occur over both time (often called *concept drift*) and space (geo-location).

Strategies for dealing with non-IID data. The above taxonomy of the many regimes of non-IID data partitions naturally leads to the question of what should the objective function of the DNN model be? In our study, we have focused on obtaining a global model that minimizes an objective function over the union of all the data. An alternative objective function might instead include some notion of “fairness” among the partitions in the final accuracy on their local data. There could also be different strategies for treating different non-IID regimes.

As noted in Section 8, multi-task learning approaches have been proposed for jointly training local models for each partition, but a global model is essential whenever a local model is unavailable or ineffective. A hybrid approach

would be to train a “base” global model that can be quickly “specialized” to local data via a modest amount of further training on that local data. This approach would be useful for differences across space and time. For example, a global model trained under normal circumstances could be quickly adapted to natural disaster settings such as hurricanes, flash floods and forest fires.

As one proceeds down the path towards more local/specialized models, it may make sense to cluster partitions that hold similar data, with one model for each cluster. The goal is to avoid a proliferation of too many models that must be trained, stored, and maintained over time.

Finally, another alternative for handling non-IID data partitions is to use multi-modal training that combines DNNs with key attributes about the data partition pertaining to its geo-location. A challenge with this approach is determining what the attributes should be, in order to have an accurate yet reasonably compact model (otherwise, in the extreme, the model could devolve into local models for each geo-location).

10 CONCLUSION

As most timely and relevant ML data are generated at different places, decentralized learning provides an important path for ML applications to leverage these decentralized data. However, decentralized data are often generated at different contexts, which leads to a heavily understudied problem: *non-IID training data partitions*. We conduct a detailed empirical study of this problem, revealing three key findings. First, we show that training over non-IID data partitions is a fundamental and pervasive problem for decentralized learning, as all decentralized learning algorithms in our study suffer major accuracy loss in the Non-IID setting. Second, we find that DNNs with batch normalization are particularly vulnerable in the Non-IID setting, with even the most communication-heavy approach being unable to retain model quality. We further discuss the cause and potential solution to this problem. Third, we show that the difficulty level of the non-IID data problem varies greatly with the degree of deviation from IID. Based on these findings, we present SkewScout, a system-level approach to minimizing communication while retaining model quality even under non-IID data. We hope that the findings and insights in this paper, as well as our open source code, will spur further research into the fundamental and important problem of non-IID data in decentralized learning.

REFERENCES

- Ba, L. J., Kiros, J. R., and Hinton, G. E. Layer normalization. *CoRR*, abs/1607.06450, 2016.
- Bjorck, N., Gomes, C. P., Selman, B., and Weinberger, K. Q. Understanding batch normalization. In *NeurIPS*, 2018.
- Chen, T., Li, M., Li, Y., Lin, M., Wang, N., Wang, M., Xiao, T., Xu, B., Zhang, C., and Zhang, Z. MXNet: A flexible and efficient machine learning library for heterogeneous distributed systems. *CoRR*, abs/1512.01274, 2015.
- Chilimbi, T. M., Suzue, Y., Apacible, J., and Kalyanaraman, K. Project Adam: Building an efficient and scalable deep learning training system. In *OSDI*, 2014.
- Cui, H., Tumanov, A., Wei, J., Xu, L., Dai, W., Haber-Kucharsky, J., Ho, Q., Ganger, G. R., Gibbons, P. B., Gibson, G. A., and Xing, E. P. Exploiting iterative-ness for parallel ML computations. In *SoCC*, 2014. Software available at <https://github.com/cuihenggang/iterstore>.
- Cui, H., Zhang, H., Ganger, G. R., Gibbons, P. B., and Xing, E. P. GeePS: Scalable deep learning on distributed GPUs with a GPU-specialized parameter server. In *EuroSys*, 2016. Software available at <https://github.com/cuihenggang/geeps>.
- Dean, J., Corrado, G., Monga, R., Chen, K., Devin, M., Le, Q. V., Mao, M. Z., Ranzato, M., Senior, A. W., Tucker, P. A., Yang, K., and Ng, A. Y. Large scale distributed deep networks. In *NIPS*, 2012.
- Goodfellow, I. J., Pouget-Abadie, J., Mirza, M., Xu, B., Warde-Farley, D., Ozair, S., Courville, A. C., and Bengio, Y. Generative adversarial nets. In *NIPS*, 2014.
- Goyal, P., Dollár, P., Girshick, R. B., Noordhuis, P., Wesolowski, L., Kyrola, A., Tulloch, A., Jia, Y., and He, K. Accurate, large minibatch SGD: training ImageNet in 1 hour. *CoRR*, abs/1706.02677, 2017.
- He, K., Zhang, X., Ren, S., and Sun, J. Deep residual learning for image recognition. In *CVPR*, 2016.
- Ho, Q., Cipar, J., Cui, H., Lee, S., Kim, J. K., Gibbons, P. B., Gibson, G. A., Ganger, G. R., and Xing, E. P. More effective distributed ML via a stale synchronous parallel parameter server. In *NIPS*, 2013.
- Hochreiter, S. and Schmidhuber, J. Long short-term memory. *Neural Computation*, 9(8), 1997.
- Hsieh, K., Harlap, A., Vijaykumar, N., Konomis, D., Ganger, G. R., Gibbons, P. B., and Mutlu, O. Gaia: Geo-distributed machine learning approaching LAN speeds. In *NSDI*, 2017.
- Huang, G. B., Ramesh, M., Berg, T., and Learned-Miller, E. Labeled faces in the wild: A database for studying face recognition in unconstrained environments. Technical Report 07-49, University of Massachusetts, Amherst, October 2007.
- Ioffe, S. Batch renormalization: Towards reducing minibatch dependence in batch-normalized models. In *NIPS*, 2017.
- Ioffe, S. and Szegedy, C. Batch normalization: Accelerating deep network training by reducing internal covariate shift. In *ICML*, 2015.
- Jaggi, M., Smith, V., Takác, M., Terhorst, J., Krishnan, S., Hofmann, T., and Jordan, M. I. Communication-efficient distributed dual coordinate ascent. In *NIPS*, 2014.
- Jia, Y., Shelhamer, E., Donahue, J., Karayev, S., Long, J., Girshick, R. B., Guadarrama, S., and Darrell, T. Caffe: Convolutional architecture for fast feature embedding. *CoRR*, 2014.

- Krizhevsky, A. Learning multiple layers of features from tiny images. Technical report, University of Toronto, 2009.
- Krizhevsky, A., Sutskever, I., and Hinton, G. E. ImageNet classification with deep convolutional neural networks. In *NIPS*, 2012.
- LeCun, Y., Bottou, L., Bengio, Y., Haffner, P., et al. Gradient-based learning applied to document recognition. *Proceedings of the IEEE*, 86(11), 1998.
- Li, M., Andersen, D. G., Park, J. W., Smola, A. J., Ahmed, A., Josifovski, V., Long, J., Shekita, E. J., and Su, B. Scaling distributed machine learning with the parameter server. In *OSDI*, 2014a.
- Li, M., Andersen, D. G., Smola, A. J., and Yu, K. Communication efficient distributed machine learning with the parameter server. In *NIPS*, 2014b.
- Lin, Y., Han, S., Mao, H., Wang, Y., and Dally, W. J. Deep gradient compression: Reducing the communication bandwidth for distributed training. In *ICLR*, 2018.
- Low, Y., Gonzalez, J., Kyrola, A., Bickson, D., Guestrin, C., and Hellerstein, J. M. Distributed GraphLab: A framework for machine learning in the cloud. *Vldb*, 2012.
- McMahan, B., Moore, E., Ramage, D., Hampson, S., and y Arcas, B. A. Communication-efficient learning of deep networks from decentralized data. In *AISTATS*, 2017.
- Neiswanger, W., Wang, C., and Xing, E. P. Asymptotically exact, embarrassingly parallel MCMC. In *UAI*, 2014.
- Pascanu, R., Mikolov, T., and Bengio, Y. On the difficulty of training recurrent neural networks. In *ICML*, 2013.
- Rakhlin, A., Shamir, O., and Sridharan, K. Making gradient descent optimal for strongly convex stochastic optimization. In *ICML*, 2012.
- Recht, B., Ré, C., Wright, S. J., and Niu, F. Hogwild: A lock-free approach to parallelizing stochastic gradient descent. In *NIPS*, 2011.
- Russakovsky, O., Deng, J., Su, H., Krause, J., Satheesh, S., Ma, S., Huang, Z., Karpathy, A., Khosla, A., Bernstein, M., Berg, A. C., and Fei-Fei, L. ImageNet large scale visual recognition challenge. *IJCV*, 2015.
- Russell, S. J. and Norvig, P. *Artificial Intelligence: A Modern Approach*. Malaysia; Pearson Education Limited, 2016.
- Salimans, T. and Kingma, D. P. Weight normalization: A simple reparameterization to accelerate training of deep neural networks. In *NIPS*, 2016.
- Santurkar, S., Tsipras, D., Ilyas, A., and Madry, A. How does batch normalization help optimization? In *NeurIPS*, 2018.
- Shalev-Shwartz, S. and Zhang, T. Stochastic dual coordinate ascent methods for regularized loss. *JMLR*, 14(1), 2013.
- Shamir, O., Srebro, N., and Zhang, T. Communication-efficient distributed optimization using an approximate Newton-type method. In *ICML*, 2014.
- Shokri, R. and Shmatikov, V. Privacy-preserving deep learning. In *CCS*, 2015.
- Smith, V., Chiang, C., Sanjabi, M., and Talwalkar, A. S. Federated multi-task learning. In *NIPS*, 2017.
- Szegedy, C., Liu, W., Jia, Y., Sermanet, P., Reed, S. E., Anguelov, D., Erhan, D., Vanhoucke, V., and Rabinovich, A. Going deeper with convolutions. In *CVPR*, 2015.
- Szegedy, C., Vanhoucke, V., Ioffe, S., Shlens, J., and Wojna, Z. Rethinking the inception architecture for computer vision. In *CVPR*, 2016.
- Takác, M., Bijral, A. S., Richtárik, P., and Srebro, N. Mini-batch primal and dual methods for SVMs. In *ICML*, 2013.
- Tang, H., Lian, X., Yan, M., Zhang, C., and Liu, J. D^2 : Decentralized training over decentralized data. In *ICML*, 2018.
- Valiant, L. G. A bridging model for parallel computation. *Commun. ACM*, 1990.
- Van Laarhoven, P. J. and Aarts, E. H. Simulated annealing. In *Simulated Annealing: Theory and Applications*. Springer, 1987.
- Wen, Y., Zhang, K., Li, Z., and Qiao, Y. A discriminative feature learning approach for deep face recognition. In *ECCV*, 2016.
- Wu, Y. and He, K. Group normalization. In *ECCV*, 2018.
- Yi, D., Lei, Z., Liao, S., and Li, S. Z. Learning face representation from scratch. *CoRR*, abs/1411.7923, 2014.
- Zhang, Y. and Lin, X. DiSCO: Distributed optimization for self-concordant empirical loss. In *ICML*, 2015.
- Zhang, Y., Duchi, J. C., and Wainwright, M. J. Communication-efficient algorithms for statistical optimization. *JMLR*, 2013.
- Zhao, Y., Li, M., Lai, L., Suda, N., Civin, D., and Chandra, V. Federated learning with non-IID data. *CoRR*, abs/1806.00582, 2018.
- Zinkevich, M., Weimer, M., Smola, A. J., and Li, L. Parallelized stochastic gradient descent. In *NIPS*, 2010.

APPENDIX

A DETAILS OF DECENTRALIZED LEARNING ALGORITHMS

This section presents pseudocode for Gaia, FederatedAveraging and DeepGradientCompression.

Algorithm 1 Gaia (Hsieh et al., 2017) on node k for vanilla momentum SGD

Input: initial weights $w_0 = \{w_0[0], \dots, w_0[M]\}$

Input: K data partitions (or data centers); initial significance threshold T_0

Input: local minibatch size B ; momentum m ; learning rate η ; local dataset \mathcal{X}_k

```

1:  $u_0^k \leftarrow 0; v_0^k \leftarrow 0$ 
2:  $w_0^k \leftarrow w_0$ 
3: for  $t = 0, 1, 2, \dots$  do
4:    $b \leftarrow$  (sample  $B$  data samples from  $\mathcal{X}_k$ )
5:    $u_{t+1}^k \leftarrow m \cdot u_t^k - \eta \cdot \nabla f(w_t^k, b)$ 
6:    $w_{t+1}^k \leftarrow w_t^k + u_{t+1}^k$ 
7:    $v_{t+1}^k \leftarrow v_t^k + u_{t+1}^k$  ▷ Accumulate weight updates
8:   for  $j = 0, 1, \dots, M$  do
9:      $S \leftarrow \|\frac{v_{t+1}^k}{w_{t+1}^k}\| > T_t$  ▷ Check if accumulated updates are significant
10:     $\tilde{v}_{t+1}^k[j] \leftarrow v_{t+1}^k[j] \odot S$  ▷ Share significant updates with other  $P_k$ 
11:     $v_{t+1}^k[j] \leftarrow v_{t+1}^k[j] \odot \neg S$  ▷ Clear significant updates locally
12:  end for
13:  for  $i = 0, 1, \dots, K; i \neq k$  do
14:     $w_{t+1}^k \leftarrow w_{t+1}^k + \tilde{v}_{t+1}^i$  ▷ Apply significant updates from other  $P_k$ 
15:  end for
16:   $T_{t+1} \leftarrow \text{update\_threshold}(T_t)$  ▷ Decreases whenever the learning rate decreases
17: end for

```

Algorithm 2 FederatedAveraging (McMahan et al., 2017) on node k for vanilla momentum SGD

Input: initial weights w_0 ; K data partitions (or clients)

Input: local minibatch size B ; local iteration number $Iter_{Local}$

Input: momentum m ; learning rate η ; local dataset \mathcal{X}_k

```

1:  $u^k \leftarrow 0$ 
2: for  $t = 0, 1, 2, \dots$  do
3:    $w_t^k \leftarrow w_t$  ▷ Get the latest weight from the server
4:   for  $i = 0, \dots, Iter_{Local}$  do
5:      $b \leftarrow$  (sample  $B$  data samples from  $\mathcal{X}_k$ )
6:      $u^k \leftarrow m \cdot u^k - \eta \cdot \nabla f(w_t^k, b)$ 
7:      $w_t^k \leftarrow w_t^k + u^k$ 
8:   end for
9:   all_reduce:  $w_{t+1} \leftarrow \sum_{k=1}^K \frac{1}{K} w_t^k$  ▷ Average weights among all partitions
10: end for

```

Algorithm 3 DeepGradientCompression (Lin et al., 2018) on node k for vanilla momentum SGD

Input: initial weights $w_0 = \{w_0[0], \dots, w_0[M]\}$
Input: K data partitions (or data centers); $s\%$ update sparsity
Input: local minibatch size B ; momentum m ; learning rate η ; local dataset \mathcal{X}_k

```

1:  $u_0^k \leftarrow 0; v_0^k \leftarrow 0$ 
2: for  $t = 0, 1, 2, \dots$  do
3:    $b \leftarrow$  (sample  $B$  data samples from  $\mathcal{X}_k$ )
4:    $g_{t+1}^k \leftarrow -\eta \cdot \nabla f(w_t, b)$ 
5:    $g_{t+1}^k \leftarrow \text{gradient\_clipping}(g_{t+1}^k)$  ▷ Gradient clipping
6:    $u_{t+1}^k \leftarrow m \cdot u_t^k + g_{t+1}^k$ 
7:    $v_{t+1}^k \leftarrow v_t^k + u_{t+1}^k$  ▷ Accumulate weight updates
8:    $T \leftarrow s\%$  of  $\|v_{t+1}^k\|$  ▷ Determine the threshold for sparsified updates
9:   for  $j = 0, 1, \dots, M$  do
10:     $S \leftarrow \|v_{t+1}^k\| > T$  ▷ Check if accumulated updates are top  $s\%$ 
11:     $\tilde{v}_{t+1}^k[j] \leftarrow v_{t+1}^k[j] \odot S$  ▷ Share top updates with other  $P_k$ 
12:     $v_{t+1}^k[j] \leftarrow v_{t+1}^k[j] \odot \neg S$  ▷ Clear top updates locally
13:     $u_{t+1}^k[j] \leftarrow u_{t+1}^k[j] \odot \neg S$  ▷ Clear the history of top updates (momentum correction)
14:   end for
15:    $w_{t+1} = w_t + \sum_{k=1}^K \tilde{v}_{t+1}^k$  ▷ Apply top updates from all  $P_k$ 
16: end for
    
```

B TRAINING PARAMETERS

Tables 3, 4, 5 list the major training parameters for all the applications, models, and datasets in our study.

Model	Minibatch size per node (5 nodes)	Momentum	Weight decay	Learning rate	Total epochs
AlexNet	20	0.9	0.0005	$\eta_0 = 0.0002$, divides by 10 at epoch 64 and 96	128
GoogLeNet	20	0.9	0.0005	$\eta_0 = 0.002$, divides by 10 at epoch 64 and 96	128
LeNet, BN-LeNet, GN-LeNet	20	0.9	0.0005	$\eta_0 = 0.002$, divides by 10 at epoch 64 and 96	128
ResNet-20	20	0.9	0.0005	$\eta_0 = 0.002$, divides by 10 at epoch 64 and 96	128

Table 3: Major training parameters for IMAGE CLASSIFICATION over CIFAR-10

Model	Minibatch size per node (8 nodes)	Momentum	Weight decay	Learning rate	Total epochs
GoogLeNet	32	0.9	0.0002	$\eta_0 = 0.0025$, polynomial decay, power = 0.5	60
ResNet-10	32	0.9	0.0001	$\eta_0 = 0.00125$, polynomial decay, power = 1	64

Table 4: Major training parameters for IMAGE CLASSIFICATION over ImageNet. Polynomial decay in the learning rate means $\eta = \eta_0 \cdot (1 - \frac{\text{iter}}{\text{max_iter}})^{\text{power}}$.

Model	Minibatch size per node (4 nodes)	Momentum	Weight decay	Learning rate	Total epochs
center-loss	64	0.9	0.0005	$\eta_0 = 0.025$, divides by 10 at epoch 4 and 6	7

Table 5: Major training parameters for FACE RECOGNITION over CASIA-WebFace.

C MORE ALGORITHM HYPER-PARAMETER RESULTS

§4.2 presents hyper-parameter sensitivity results for Gaia on two DNNs. Here, we expand the sensitivity study to show more results for Gaia, FederatedAveraging and DeepGradientCompression. We make the same observation as §4.2 for these algorithms. The results are shown in Tables 6, 7 and 8.

Configuration	LeNet		ResNet20	
	IID	Non-IID	IID	Non-IID
BSP	77.4%	76.6%	83.7%	44.3%
$T_0 = 2\%$	76.9%	52.6%	83.1%	48.0%
$T_0 = 5\%$	74.6%	10.0%	83.2%	43.1%
$T_0 = 10\%$	76.7%	10.0%	84.0%	45.1%
$T_0 = 20\%$	77.7%	10.0%	83.6%	38.9%
$T_0 = 30\%$	78.6%	10.0%	81.3%	39.4%
$T_0 = 40\%$	78.3%	10.1%	82.1%	28.5%
$T_0 = 50\%$	78.0%	10.0%	77.3%	28.4%

Table 6: Top-1 validation accuracy (CIFAR-10) varying Gaia’s T_0 hyper-parameter for LeNet and ResNet20. The configurations with more than 2% accuracy loss from BSP in the IID setting are highlighted. Note that larger settings for T_0 mean significantly greater communication savings.

Configuration	AlexNet		GoogLeNet		LeNet		ResNet20	
	IID	Non-IID	IID	Non-IID	IID	Non-IID	IID	Non-IID
BSP	74.9%	75.0%	79.1%	78.9%	77.4%	76.6%	83.7%	44.3%
$Iter_{Local} = 5$	73.7%	62.8%	75.8%	68.9%	79.7%	67.3%	73.6%	31.3%
$Iter_{Local} = 10$	73.5%	60.1%	76.4%	64.8%	79.3%	63.2%	73.4%	28.0%
$Iter_{Local} = 20$	73.4%	59.4%	76.3%	64.0%	79.1%	10.1%	73.8%	28.1%
$Iter_{Local} = 50$	73.5%	56.3%	75.9%	59.6%	79.2%	55.6%	74.0%	26.3%
$Iter_{Local} = 200$	73.7%	53.2%	76.8%	52.9%	79.4%	54.2%	75.7%	27.3%
$Iter_{Local} = 500$	73.0%	24.0%	76.8%	20.8%	79.6%	19.4%	74.1%	24.0%
$Iter_{Local} = 1000$	73.4%	23.9%	76.1%	20.9%	78.3%	19.0%	74.3%	22.8%

Table 7: Top-1 validation accuracy (CIFAR-10) with various FederatedAveraging hyper-parameters. The configurations that lose more than 2% accuracy are highlighted. Note that larger settings for $Iter_{Local}$ mean significantly greater communication savings.

Configuration	AlexNet		GoogLeNet		LeNet		ResNet20	
	IID	Non-IID	IID	Non-IID	IID	Non-IID	IID	Non-IID
BSP	74.9%	75.0%	79.1%	78.9%	77.4%	76.6%	83.7%	44.3%
$E_{warm} = 8$	75.5%	72.3%	78.3%	10.0%	80.3%	47.2%	10.0%	10.0%
$E_{warm} = 4$	75.5%	75.7%	79.4%	61.6%	10.0%	47.3%	10.0%	10.0%
$E_{warm} = 3$	75.9%	74.9%	78.9%	75.7%	64.9%	50.5%	10.0%	10.0%
$E_{warm} = 2$	75.7%	76.7%	79.0%	58.7%	10.0%	47.5%	10.0%	10.0%
$E_{warm} = 1$	75.4%	77.9%	78.6%	74.7%	10.0%	39.9%	10.0%	10.0%

Table 8: Top-1 validation accuracy (CIFAR-10) with various DeepGradientCompression hyper-parameters. The configurations that lose more than 2% accuracy are highlighted. Note that smaller settings for E_{warm} mean significantly greater communication savings.